

Electronic Supplementary Information:

Enhanced Photovoltaic Performance of Ultrathin Si Solar

Cells via Semiconductor Nanocrystal Sensitization:

Energy Transfer vs. Optical Coupling Effects

Son Hoang,¹ Ahsan Ashraf,^{2,3} Matthew D. Eisaman,^{2,3,4} Dmytro Nykypanchuk,^{1,}
and Chang-Yong Nam^{1,*}*

¹ Center for Functional Nanomaterials, Brookhaven National Laboratory, Upton, New York
11973, United States

² Sustainable Energy Technologies Department, Brookhaven National Laboratory, Upton, New
York 11973, United States

³ Department of Physics and Astronomy, Stony Brook University, Stony Brook, New York
11794, United States

⁴ Department of Electrical and Computer Engineering, Stony Brook University, Stony Brook,
New York 11794, United States

*Corresponding authors: dnykypan@bnl.gov (D.N.), cynam@bnl.gov (C.-Y.N.)

Theoretical calculation of energy transfer (ET) efficiency

Readers are encouraged to read the article by Nguyen et al. (ACS Nano **6**, 5574-5582 (2012)) for more details. In vacuum, the decay rate (Γ_0) and the lifetime ($1/\Gamma_0$) of an ideal point electric dipole emitter due to radiative transitions are determined from

$$\Gamma_0 = \frac{k^3 |\mathbf{p}|^2}{3\pi\epsilon_0\hbar} \quad (1)$$

where $k = \omega/c = 2\pi/\lambda$ is the emission wavenumber and \mathbf{p} is the effective dipole transition moment. When a random-oriented dipole is placed at a distance z from a planar surface of a stratified substrate with each layer having frequency-dependent complex dielectric function $\epsilon(\omega) = \epsilon'(\omega) + i\epsilon''(\omega)$, the electromagnetic decay rate (Γ) can be calculated from the equation:

$$\frac{\Gamma}{\Gamma_0} = 1 + l(0, \infty) \quad (2)$$

$$\text{with } l(a, b) = \text{Re} \int_a^b \frac{s ds}{2\sqrt{1-s^2}} [(2s^2 - 1)r^{(p)}(s) + r^{(s)}(s)] \exp(2ikz\sqrt{1-s^2}) \quad (3)$$

where $r^{(p)}$ and $r^{(s)}$ are the reflection coefficients for p- and s-polarized waves, respectively, containing the information on the dielectric function $\epsilon(\omega)$ of the substrate. In our case, the substrate structure takes into account all possible interfaces such as air/quantum dot (NC), air/ AlO_x , air/ SiO_2 , NC/ AlO_x , NC/ SiO_2 , $\text{AlO}_x/\text{SiO}_2$, and SiO_2/Si for calculation of reflection and transmission coefficients. Since, the in-plane (parallel to the interface) component of the wave vector are conserved after reflection/refraction at planar interfaces, the variable s in the integration in equation (3) can be related to the magnitude k_{\parallel} of the in-plane components and the vacuum wavenumber k_0 : $k_{\parallel}(s) = sk_0$. Therefore, the normal component of the wave vector, k_{zi} , in the i^{th} layer is determined by the dielectric function ϵ_i of that layer

$$k_{zi}^2(s) = (\varepsilon_i - s^2)k_0^2 \quad (4)$$

In low absorption ($\varepsilon'' \ll \varepsilon'$) dielectric system, the integration in equation (2) can be separated into parts limited by the values of refractive indices $n_i(\cong \sqrt{\varepsilon'})$ of the layers to distinguish between ‘propagating’ (real or near real k_{zi} values) and ‘evanescent’ (imaginary k_{zi} values) characteristics. Since AlO_x deposited by atomic layer deposition (ALD) and SiO_2 layers have similar refractive indices (~ 1.5) at the wavelength of interest, ~ 605 nm, we treated stack of AlO_x and SiO_2 as a single spacer layer having refractive index of 1.5. From the equation (4), it can be seen that the contributions $\Gamma_v/\Gamma_0 = 1 + l(0,1)$ and $\Gamma_{spacer}/\Gamma_0 = l(1,1.5)$ of equation (2) correspond to the decay into photons with the propagating characteristics into the vacuum and spacer, respectively. Since the absorption depth of $\lambda_0 = 605$ nm is ~ 3 μm , much larger than thickness of the Si membrane, re-absorption of these photons in Si is negligible and we consider Γ_v and Γ_{spacer} as lost during energy transfer (ET). The contribution $\Gamma_{RET}/\Gamma_0 = l(1.5, \sqrt{\varepsilon_{Si}'})$ corresponds to the decay into the electromagnetic modes which are evanescent outside slab but propagating inside Si membrane and eventually absorbed by Si due to finite value of ε_{Si}'' , thus considered as radiative ET (RET). Finally, the contribution $\Gamma_{NRET}/\Gamma_0 = l(\sqrt{\varepsilon_{Si}'}, \infty)$ does not have propagating characteristics and corresponds to nonradiative ET (NRET) due to Joule losses of the electromagnetic field in Si membrane. The ET efficiencies due to RET and NRET are given as the fraction of total decay rate (Γ), Γ_{RET}/Γ and Γ_{NRET}/Γ , respectively. The total ET efficiency is summation of RET and NRET, thus calculated as

$$\eta_{ET} = \frac{\Gamma_{RET} + \Gamma_{NRET}}{\Gamma} \quad (5)$$

Calculation of inter-NC ET efficiency

Due to negligible optical absorption of NCs at their photoluminescence wavelengths, the ET between NCs is mainly via NRET. The inter-NC NRET is due to the inhomogeneous distribution of the NC core-sizes, which is reflected in the spectral distribution of photoluminescence (PL) of NCs (Figure S4). The inter-NC NRET efficiency (Eff) is calculated using equation:

$$Eff = \frac{1}{1+(r/R_0)^6} \quad (6)$$

with r being the separation distance between NCs and R_0 being the Förster radius, i.e. the distance at which the ET efficiency is 50%.

R_0 depends on the spectra overlap integral of the donor emission spectrum with the acceptor absorption spectrum and is given by:

$$R_0^6 = \frac{9\eta_{PL}\kappa^2}{128\pi^5n^4} \int \lambda^4 F_D(\lambda)\sigma_A(\lambda)d\lambda \quad (7)$$

where η_{PL} is the PL quantum yield of the NC (~ 0.9 for our samples), κ^2 is the dipole orientational factor ($\kappa^2 = 2/3$ for randomly oriented dipoles), n is the refractive index of the medium (~ 1.5 from ellipsometry measurements), $F_D(\lambda)$ is of the donor emission spectrum normalized to an integrated value of 1, and $\sigma_A(\lambda)$ is the acceptor absorption spectrum in units of cross-sectional area. In our calculation, $F_D(\lambda)$ and $\sigma_A(\lambda)$ were extracted from the PL and UV-vis absorption measurements of the same sample with 4-monolayer NC deposited on glass to avoid any ambiguity arising from the impact of the semiconductor surface. The absorption spectrum was corrected for scattering effects using a|e - UV-Vis-IR Spectral Software. From equation (7), the Förster radius is 4.6 nm. With the average separation distance between NCs over 8 nm (the average diameter of NCs including the polymer shelf), the inter-NC ET efficiency is less than 3.5 %.

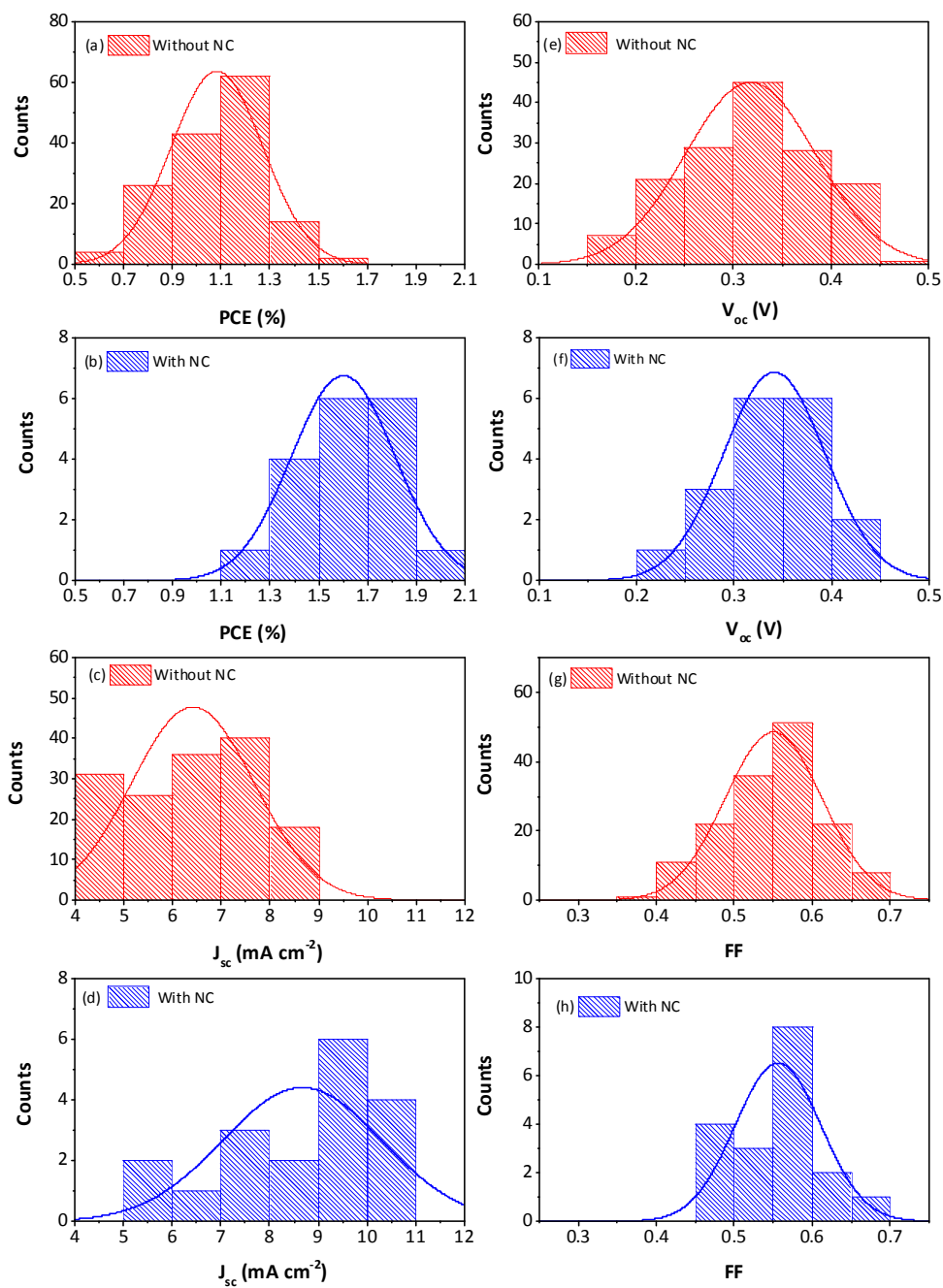


Figure S1. Histogram of photovoltaic (PV) characteristics of ultrathin Si solar cells having no AlO_x spacer, with (blue-dashed) or without (red-dashed) four monolayers of CdSe/ZnS core-shell NC energy donor.

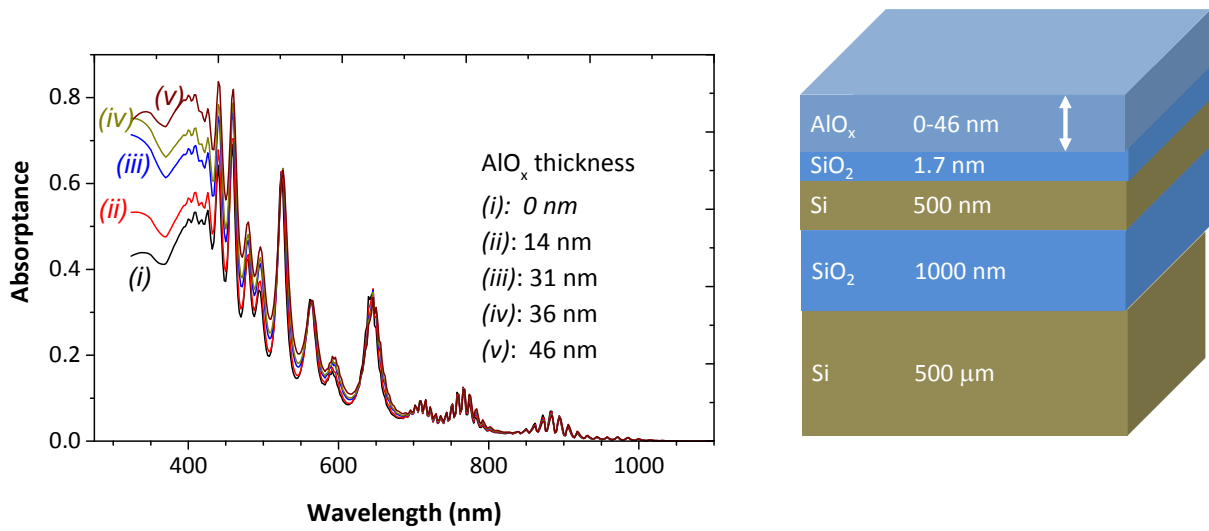


Figure S2. Simulated absorbance spectra of the Si membrane (500 nm thickness) in the silicon-on-insulator (SOI) substrate as a function of the thickness of the AlO_x layer.

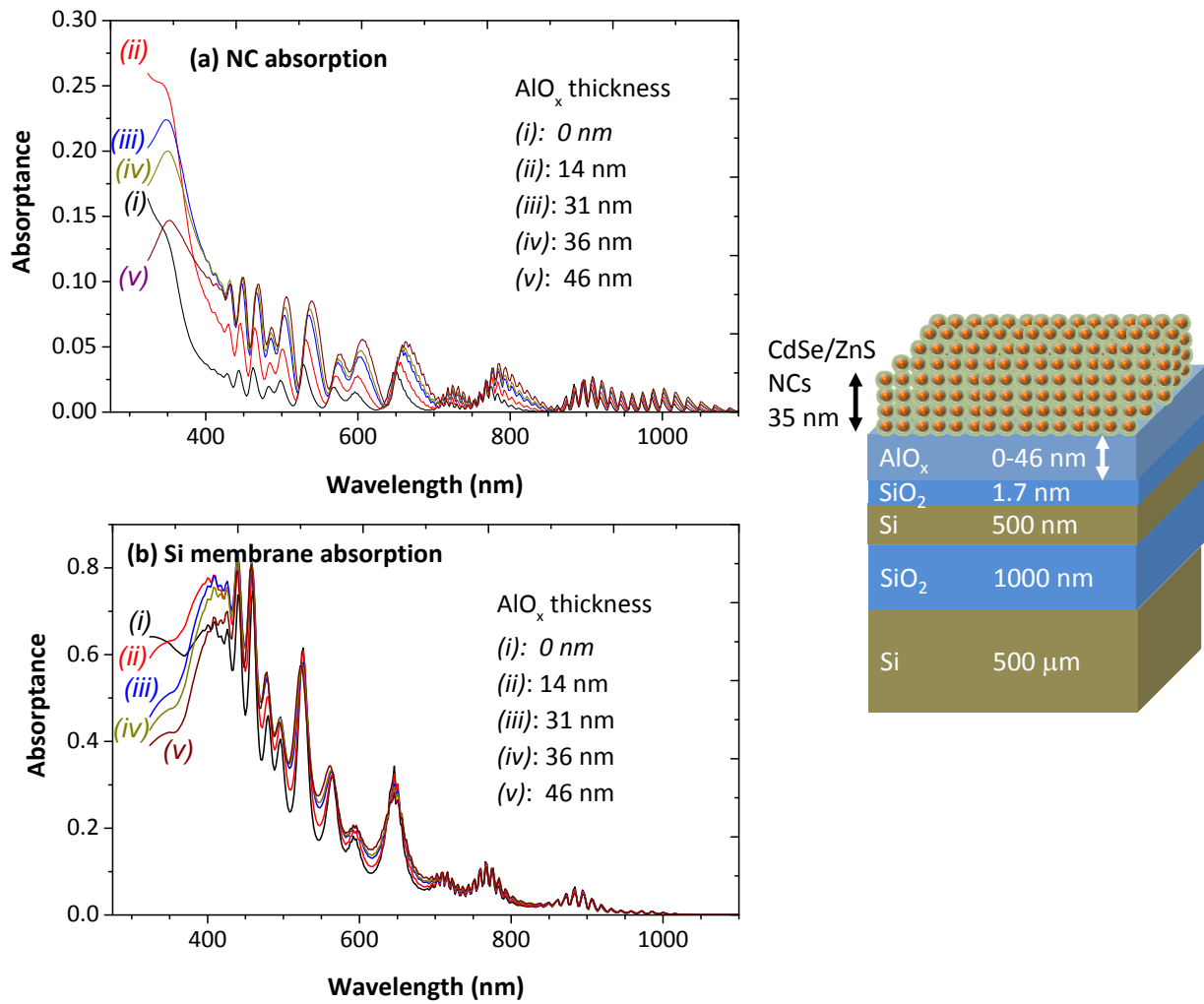


Figure S3. Simulated absorbance spectra of (A) 35 nm thick CdSe/ZnS NC layer and (B) 500 nm thick Si membrane in the device structure as a function of AlO_x thickness. It is noted that for calculating J_{ET} contributed by NC, the photocurrent integration over AM1.5G spectrum was done up to 650 nm cutoff wavelength to exclude the spurious optical absorption of NC layer appearing $\lambda > 650$ nm in the simulation.

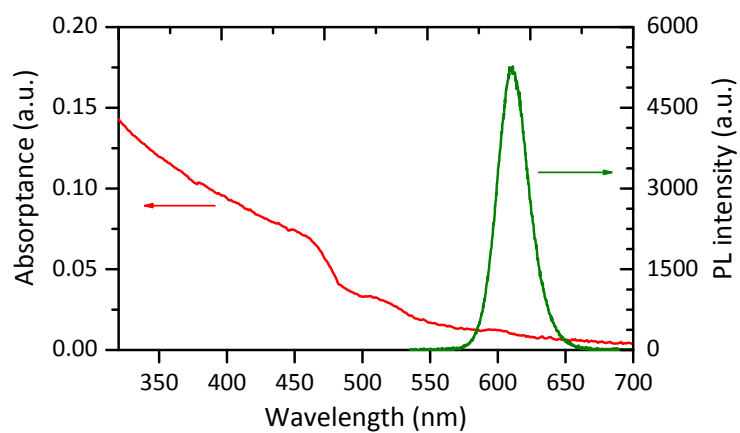


Figure S4. Measured optical absorbance and PL (excitation wavelength of 405 nm) of 35 nm thick CdSe/ZnS NC film on a glass substrate.

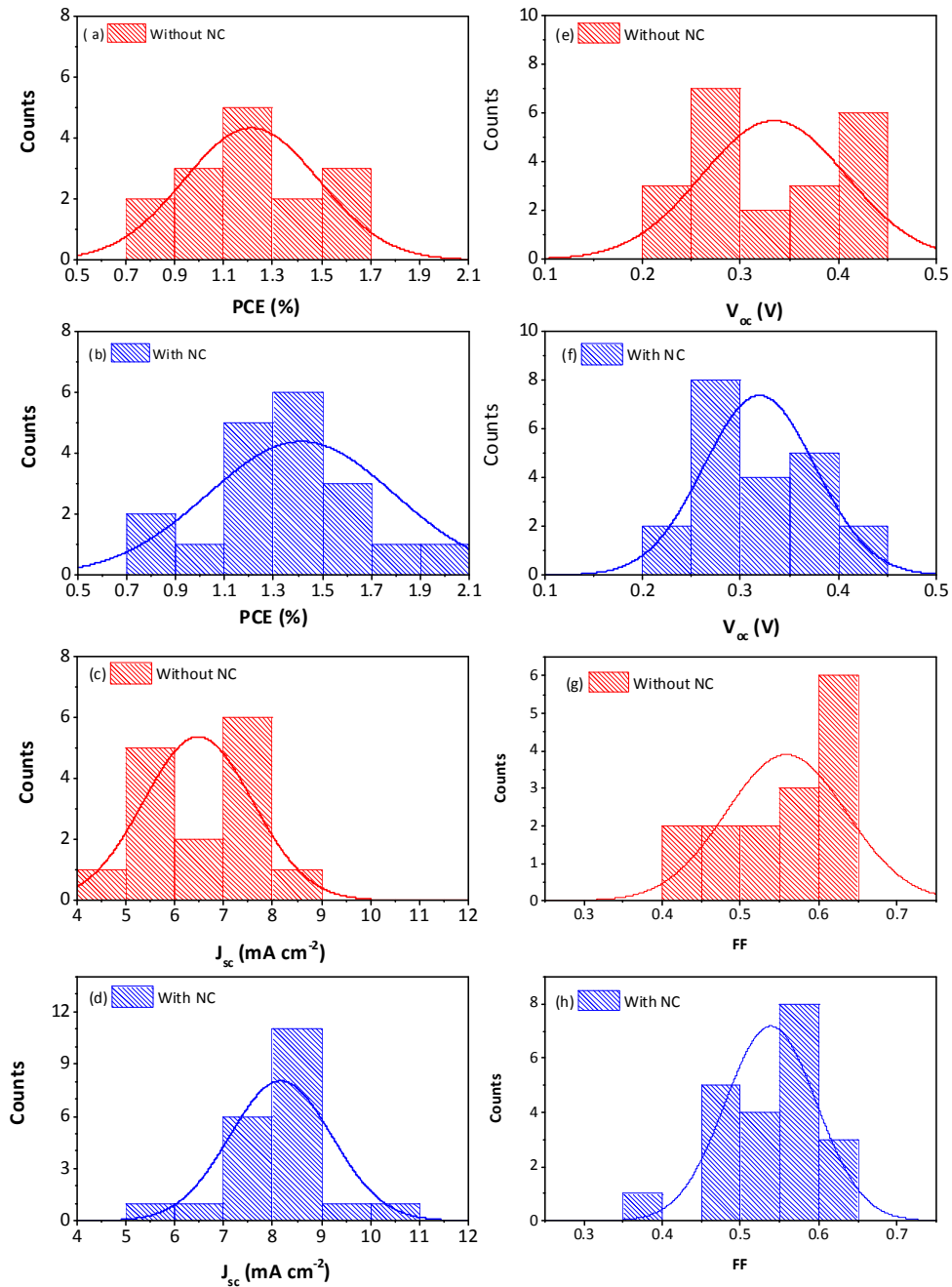


Figure S5. Histogram of PV characteristics of ultrathin Si solar cells having 14 nm thick AlO_x spacer, with (blue-dashed) or without (red-dashed) four monolayers of CdSe/ZnS core-shell NC energy donor.

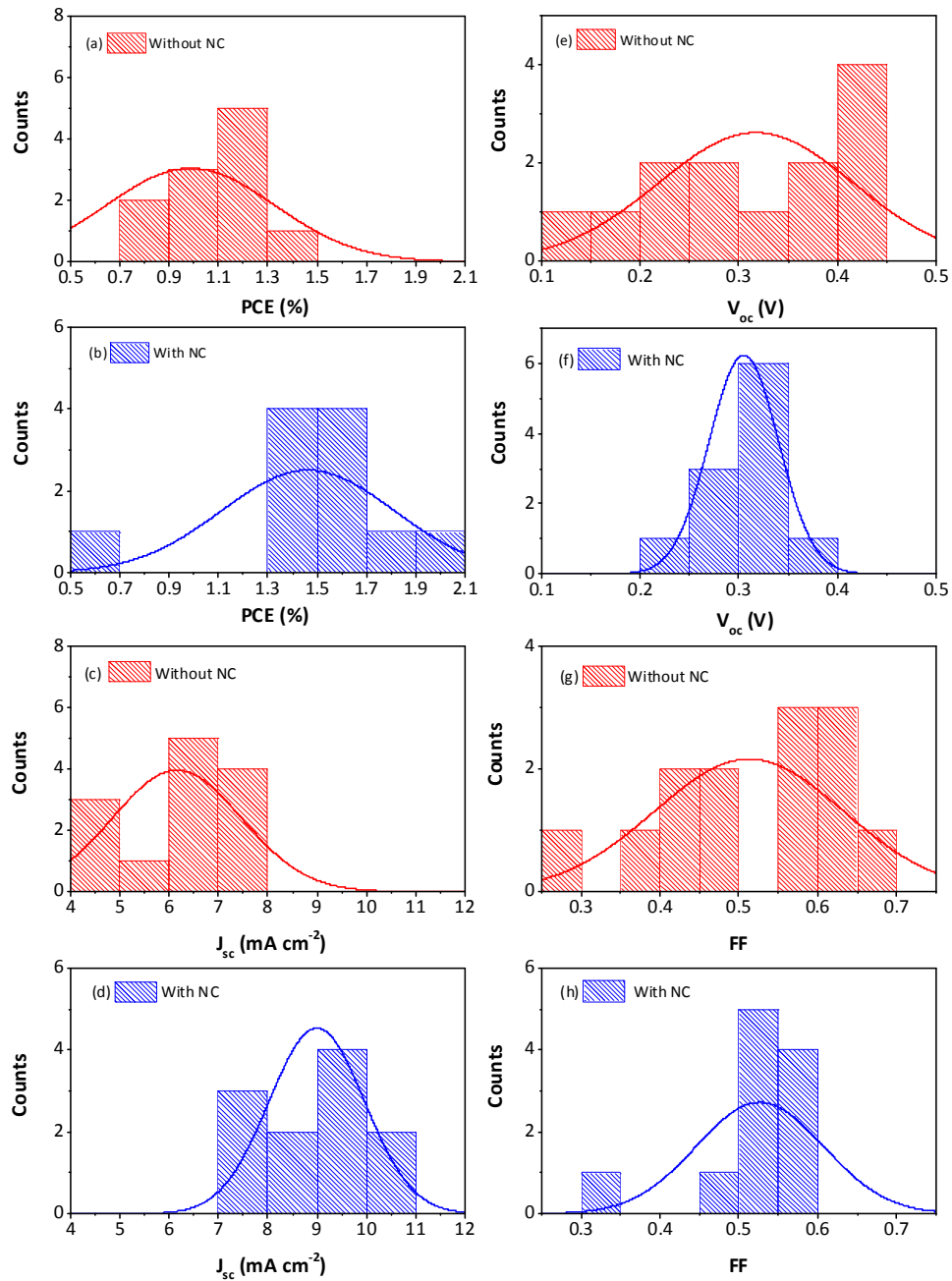


Figure S6. Histogram of PV characteristics of ultrathin Si solar cells having 31 nm thick AlO_x spacer, with (blue-dashed) or without (red-dashed) four monolayers of CdSe/ZnS core-shell NC energy donor.

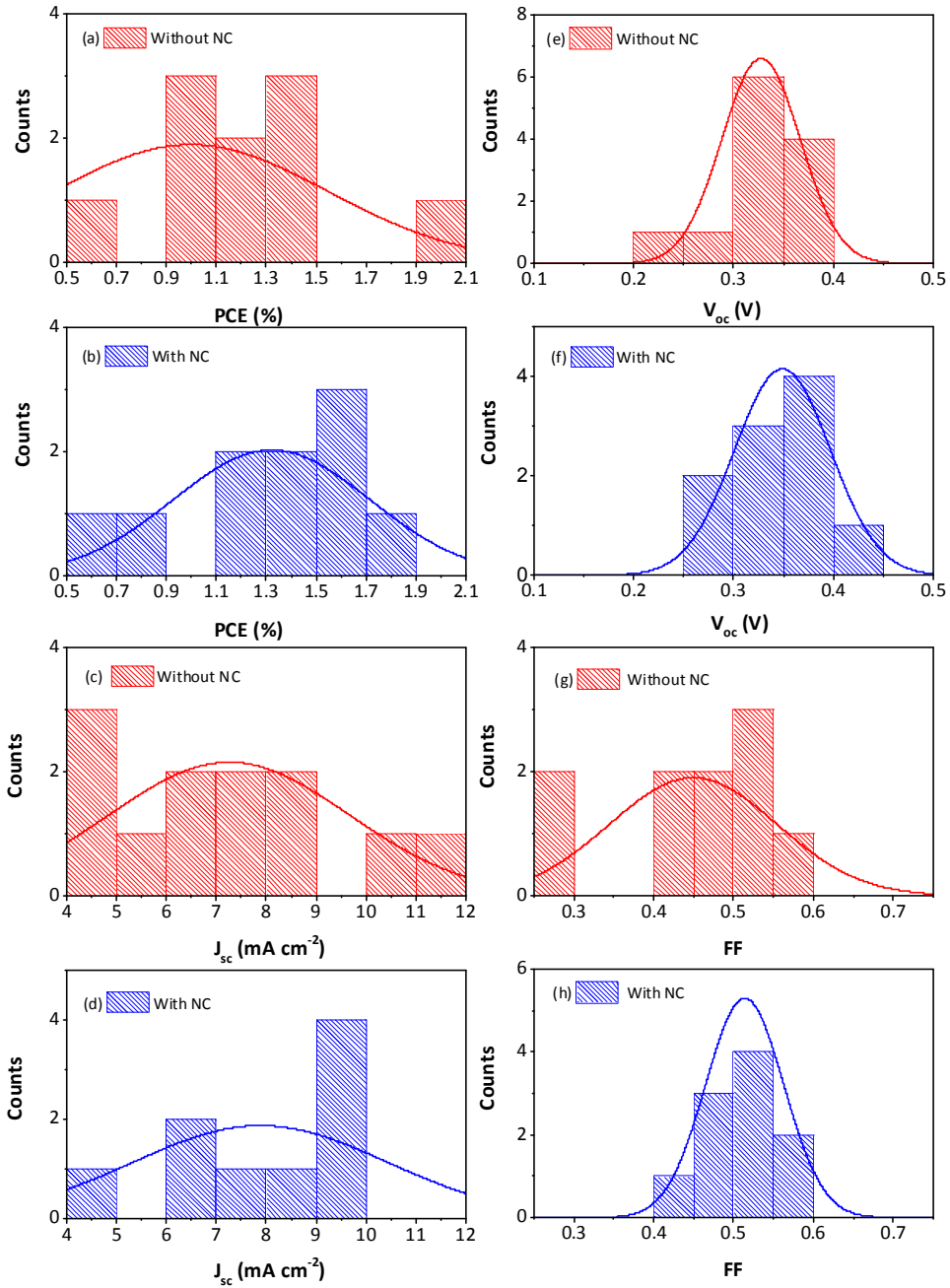


Figure S7. Histogram of PV characteristics of ultrathin Si solar cells having 36 nm thick AlO_x spacer, with (blue-dashed) or without (red-dashed) four monolayers of CdSe/ZnS core-shell NC energy donor.

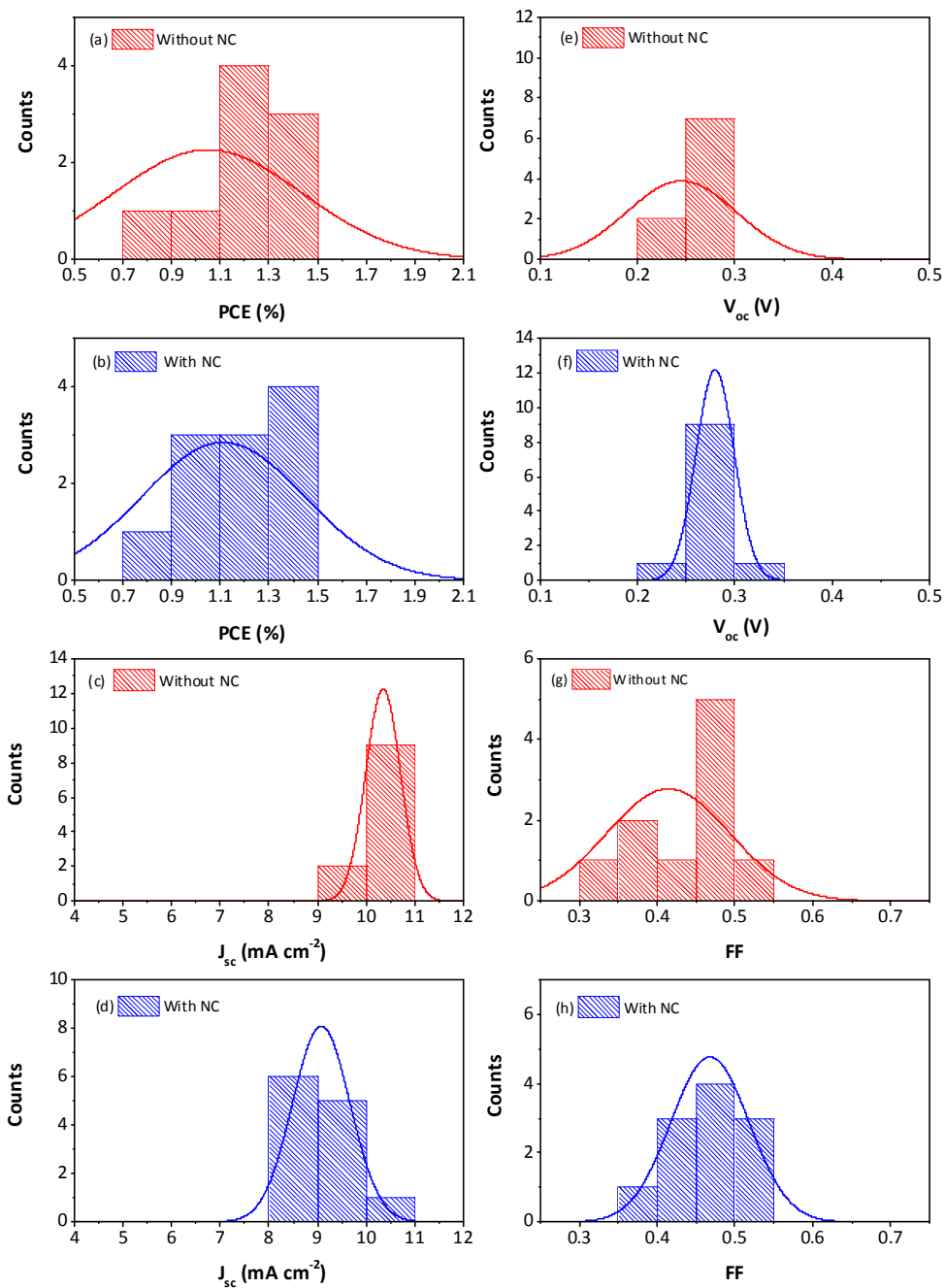


Figure S8. Histogram of PV characteristics of ultrathin Si solar cells having 46 nm thick AlO_x spacer, with (blue-dashed) or without (red-dashed) four monolayers of CdSe/ZnS core-shell NC energy donor.